

Nanoindentation and microstructure of Friction Stir Processed Die Cast Mg-Al-Zn alloy

E. Cerri, M. Cabibbo, P. Leo

A high pressure die cast (HPDC) magnesium alloy was friction stir processed (FSP) at high rotation rates with different advancing speeds. The friction stir process induced the disappearance of porosity, typical of the HPDC process, and formation of very fine grain boundary phases. Nanoindentation was used to mechanically characterize the different welded zones of interest, the thermomechanical heat affected zone (TMAZ), the stirred zone (SZ), in the advancing and the retreating side, at different sheet section depths. Aging at high temperature showed precipitates uniformly distributed inside the magnesium grains, due to the increased level of Al taken into solid solution.

Keywords: Magnesium alloys - Electron microscopy - Mechanical properties

INTRODUCTION

Friction stir processing (FSP) is a severe plastic deformation (SPD) process that was developed by Mishra et al. [1–3] as a generic tool for the microstructural modification of Al alloys and other materials. The process is based on the principle of friction stir welding (FSW) that was invented at The Welding Institute (TWI) of UK in 1991 as a solid-state joining technique [4]. The FSP process usually employs a non-consumable rotating tool comprising a threaded pin and tool shoulder to apply intense plastic deformation and frictional heating that produces significantly refined grain size due to dynamic recrystallization. Local modification of microstructure takes place within an elliptical nugget zone during the friction stir process (FSP) and specific properties are enhanced. In comparison to other metalworking processes, FSP has certain advantages, such as: (i) enhanced microstructure refinement, densification (in the case of cast and powder metallurgy materials) and homogenei-

ty in a single pass, (ii) the microstructure and mechanical properties within the nugget zone and the depth of the processed region could be controlled by the optimization of process parameters, and (iii) FSP is a “green” and energy-efficient technique since the heat input is mainly dependent on the friction and plastic deformation.

Magnesium alloys are of current interest in the transportation industry for lightweight structural applications. Recently, FSP of different magnesium alloys has been conducted to refine the microstructure and achieve improved mechanical properties [5–12].

AZ91 (Mg–9Al–1Zn) is the most popular magnesium alloy because of its superior combination of castability, mechanical specific strength, and ductility. The alloy primarily forms $Mg_{17}Al_{12}$ phase (β -phase) as precipitates in the α -Mg matrix as result of solution treatment and ageing. The β -phase is a cubic intermetallic compound. The precipitation has been found to occur continuously or discontinuously, depending on the specific heat treatment to which the alloy was subjected [14–16]. Discontinuous precipitation (DP) forms as alternate plates of secondary phase and near-equilibrium matrix phase at the high angle grain boundary sites. Continuous precipitation (CP) forms in all the remaining regions of the supersaturated matrix. The present work discusses detailed aspects of processing and the correlation of microstructure and mechanical behavior of the friction stir processed and aged high-pressure die-cast (HPDC) AZ91 alloy. The microstructure modifications and the local mechanical response, namely, hardness and elastic modulus, were here investigated. Nanoindentation was used to mechanically characterize the different welded zones of interest, the thermomechanical heat affected zone (TMAZ), the stirred zone (SZ), in the advancing and the retreating side, at different sheet section depths.

E. Cerri

*Dept. of Industrial Engineering, University of Parma,
Campus Area delle Scienze, 181/A, 43124 Parma
(ITALY), emanuela.cerri@unipr.it*

M. Cabibbo

*Dept. DIISM, Polytechnique University of Marche, Via
Brecce Bianche, 60131-Ancona (ITALY),
m.cabibbo@univpm.it*

P. Leo

*Dept. of Ingegneria dell'Innovazione, Università del
Salento, Via Arnesano, 73100-Lecce (ITALY),
paola.leo@unisalento.it*

Corresponding author:

Emanuela Cerri, emanuela.cerri@unipr.it

EXPERIMENTAL DETAILS

Material and FSP details

The AZ91 HPDC (high pressure die cast) magnesium alloy (composition in Table 1) was provided in the form of 3 mm-thick plates. The plates were friction stir processed by using pin rotation speeds, ω , of 2500 and 3000 rpm; pin travel speeds, v , were 30 and 50 mm/min. The pin had a truncated cone geometry with a shoulder diameter of 15 mm and a height of 2.3 mm.

Microstructure inspections

Light-optical (LM) overviews and detailed inspections of the FSP sheets were carried out using a Reichert-JungTM MeF-3[®] microscope. Sample surfaces were polished and etched for few seconds using a solution consisting of 10 ml acetic acid, 6 g picric acid, 10 ml distilled water in 70 ml ethanol. A ZeissTM Supra 40[®] field-emission gun scanning electron microscope (FEGSEM), operated at 10 keV, was used for the study of the inter-granular phases and the grain structure evolution induced by the FSP in the two experimental configurations. Back-scattered electrons (BSE) were used to ease the identification of the phases. To identify the intergranular phase, energy-dispersive spectra (EDS) at 10keV were used with ZAF quantitative analysis.

Mean grain size was evaluated by the line intercept method according to ASTM E112.

Nanoindentation

The elastic properties and hardness of the FSP sheets were measured by an indentation method in which a tip is pushed downward against different regions of the FSP sheet sections. By measuring the force-displacement curve, an average elastic modulus E_r (i.e. Young's modulus) and hardness H of each inspected material region was determined. Raw data analysis was performed according to the Oliver and Pharr method [17,18]. Indentation measurements were performed using a Hysitron[®] UBI[®]- I Nanoindenter, equipped with a motorized stage and a Berkovich diamond tip. The tip was calibrated with a fused quartz reference sample. A constant peak indentation force load of 1 mN was used for all the indentations. According to the round robin experimental results reported in [18], a trapezoid load function (loading time of 20 s, holding at the peak load for 60 s, followed by 3 s unloading to 10% of the peak load and a final 60 s holding at this load) was here used.

Nanoindentation measurements were performed along three different depths of the FSP sections. One was selected at 50 μm from the surface where the FSP was performed (Top); a second section depth was selected at the centerline, i.e. at the same distance from the two sheet surfaces; a third one was performed at 50 μm from the surface opposite to the one in contact with the shoulder (Bottom). All the characteristic welding zones were tested: the base metal (BM), the thermo-mechanical affected zone (TMAZ), in the advancing side (AS) and retreating side (RS), and the

Al	Zn	Mn	Si	Cu	Ni	Fe	Be	Mg
8.9	0.79	0.24	0.0093	0.0013	0.001	0.0017	3.6ppm	Bal.

Table 1 - Chemical composition of AZ91HPDC (wt. %).

Tab. 1 - Composizione chimica della lega AZ91 pressocolata.

central stirred zone (SZ). To achieve this, nanoindentation measurements were spaced 300 μm apart, starting from one side of the welded sheet, i.e. the BM, all the way through the AS-TMAZ, SZ, and TMAZ-RS to the opposite side, again in the BM, of the two welded magnesium sheets. Microhardness measurements were performed at the same depths as the nanoindentation prints and defined as Top, Center and Bottom lines. A load of 300 gf was applied each mm along a length of 30 mm with 15 s holding time.

RESULTS AND DISCUSSION

Microstructure

Figures 1 and 2 show the microstructure survey of the FSP $\omega/v = 50$ rev/mm, and $\omega/v = 83$ rev/mm, respectively. For both the FSP ω/v conditions, it appears that the grain structure decorated with intergranular eutectic regions, which characterize the BM and the TMAZ, is deeply rearranged into a recrystallized grain structure in the SZ. In particular, the SZ microstructure appears as essentially equiaxed grains with no eutectic regions. These latter were dissolved by the FSP stirring deformation before recrystallization. The FSP stirring deformation closed most of the HPDC voids that were present in the BM (Fig. 3a and 3b).

The mean grain sizes of the TMAZ and SZ, in both the FSP ω/v conditions, are listed in Table 2, where the BM mean grain size is also reported.

	BM, μm		TMAZ-AS, μm	SZ, μm	TMAZ-RS, μm
AZ91-FSP-1	8 \pm 1	Top	7.2 \pm 0.4	4.8 \pm 0.1	6.9 \pm 0.4
		Centerline	5.4 \pm 0.3	4.4 \pm 0.1	5.5 \pm 0.4
		Bottom	4.4 \pm 0.3	3.8 \pm 0.1	4.1 \pm 0.3
AZ91-FSP-2	8 \pm 1	Top	9.1 \pm 0.5	7.5 \pm 0.1	8.9 \pm 0.5
		Centerline	7.4 \pm 0.5	6.5 \pm 0.1	7.1 \pm 0.5
		Bottom	z	5.8 \pm 0.1	6.4 \pm 0.4

Table 2 - Mean grain size determined by line intercepts method (ASTM E112) at the different characteristic FSP zones of FSP-1, and FSP-2 AZ91.

Tab. 2 - Diametro medio dei grani determinato con il metodo dell'intercetta (ASTM E112) in zone caratteristiche di FSP-1 e FSP-2.

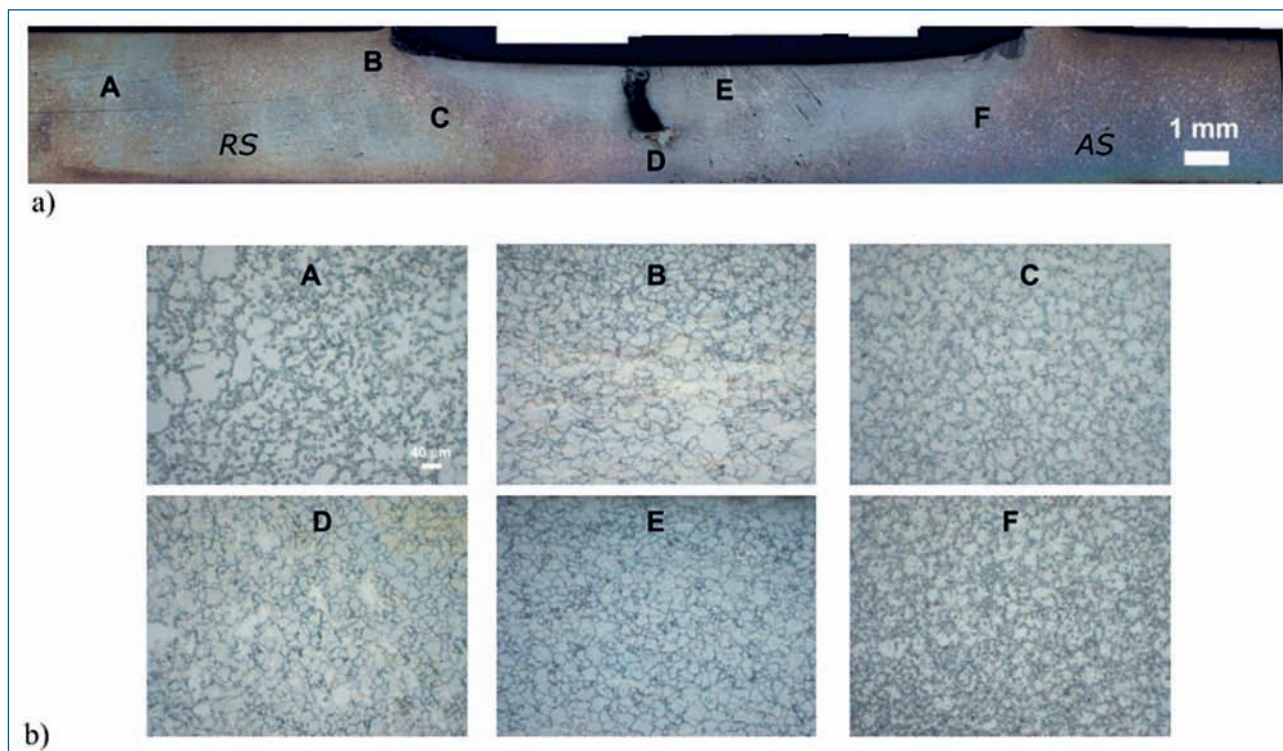


Fig. 1 - LM overview, a), and microstructure details, b) (A-to-F) of the FSP $\omega/v = 50$ rev/mm.

Fig. 1 - Macrografia a) e dettagli microstrutturali b) (da A a F) del campione FSP con $\omega/v = 50$ rev/mm.

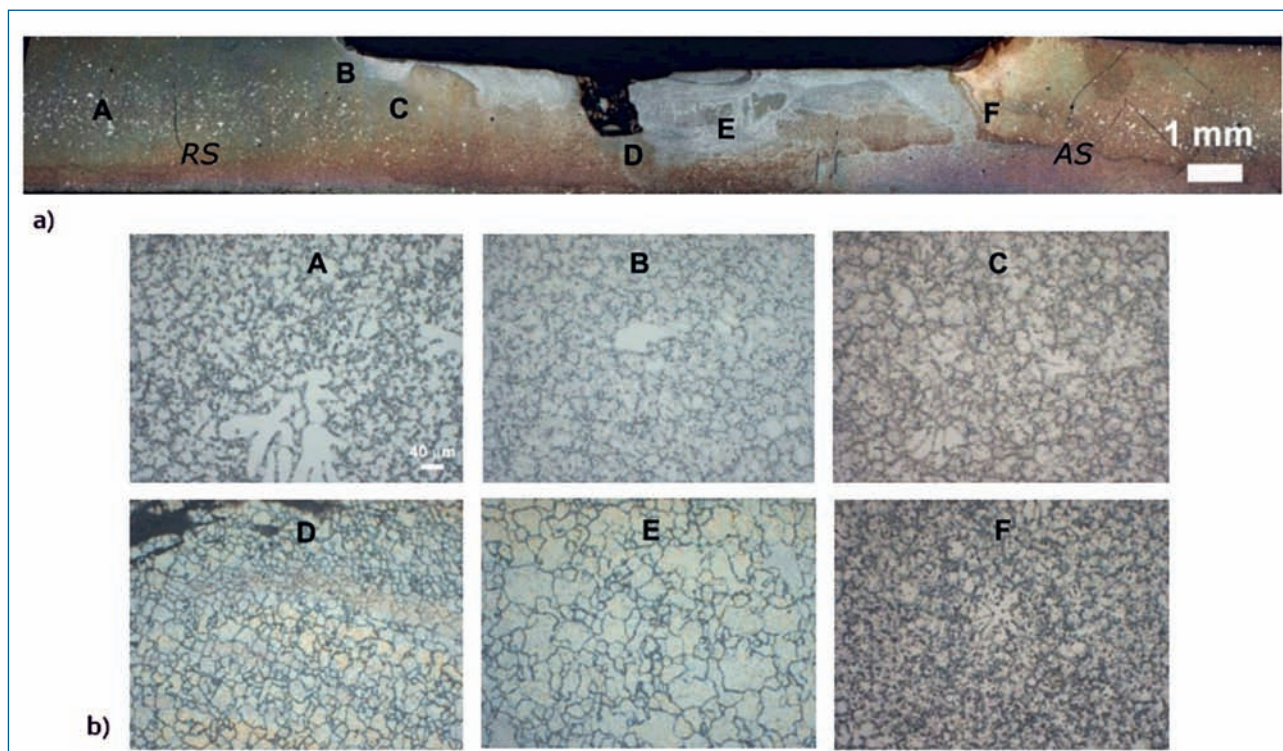


Fig. 2 - LM overview, a), and microstructure details, b) (A-to-F) of the FSP $\omega/v = 83$ rev/mm.

Fig. 2 - Macrografia a) e dettagli microstrutturali b) (da A a F) del campione FSP con $\omega/v = 83$ rev/mm.

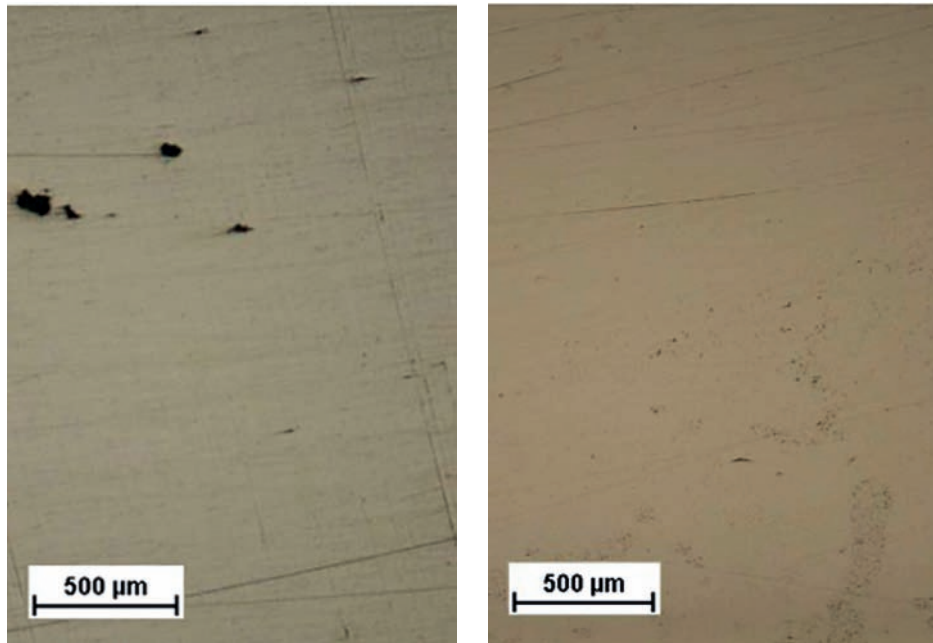


Fig. 3 - HPDC porosity in the BM (a), disappeared in (b) after FSP deformation in the SZ.

Fig. 3 - La porosità da pressocolata nel BM (a) è scomparsa in (b) dopo deformazione per FSP nella SZ.

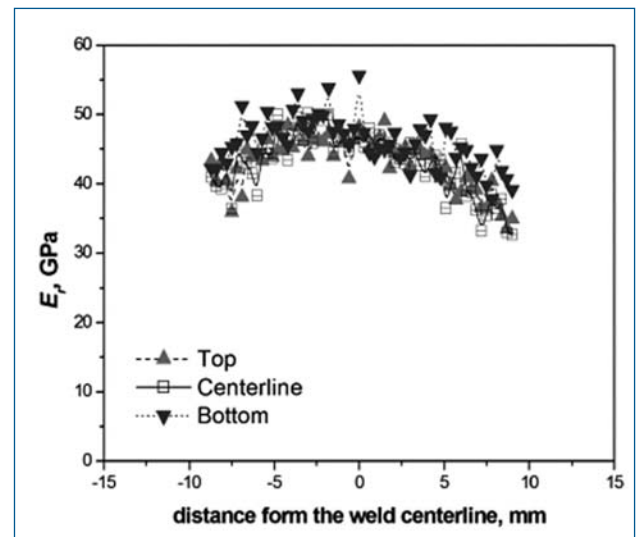
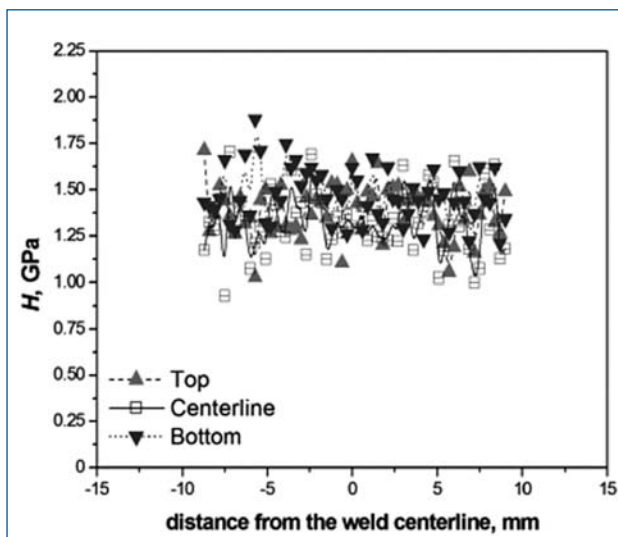


Fig. 4 - a) Hardness profile taken along three sheet section depths: 50 μm from the surface in contact with the shoulder, Top; at centerline; at 50 μm from the surface opposite to the one in contact with the shoulder. b) Local elastic modulus. FSP at $\omega/v = 50$ rev/mm.

Fig. 4 - a) Profili di microdurezza rilevati a tre profondità: a 50 μm dalla superficie in contatto con la spalla dell'utensile, Top; al centro; a 50 μm dalla superficie opposta a quella in contatto con la spalla dell'utensile. b) Modulo elastico locale. FSP a $\omega/v = 50$ rev/mm.

Mean grain sizes in both FSP-1 and FSP-2 SZ were larger in the regions close to the FSPed surface (where the shoulder passed), as compared to the centerline and the opposite surface regions. In FSP-2, with $\omega/v = 83$ rev/min, coarser grains, compared to FSP-1 ($\omega/v = 50$ rev/min) revealed in the regions close to the surface where the shoulder passed, were due to the higher thermal excursion, and longer cooling to room temperature, to which the material was subjected. This caused a grain growth of the recrystallized structure, which was more pronounced as the pin and the shoulder stayed longer in the welding pla-

tes. In fact, the recrystallized grain structure of the FSP-1 at the TMAZ and the SZ was some 30% finer than in the case of FSP-2. This is surely due to the different straining deformation experienced by the material in the two FSP settings.

Nanoindentation

Figures 4 and 5 show the nanoindentation experimental results. Figure 4a shows the hardness, H, plots and fig. 4b the elastic modulus, local Young's modulus, E_r , plots at the

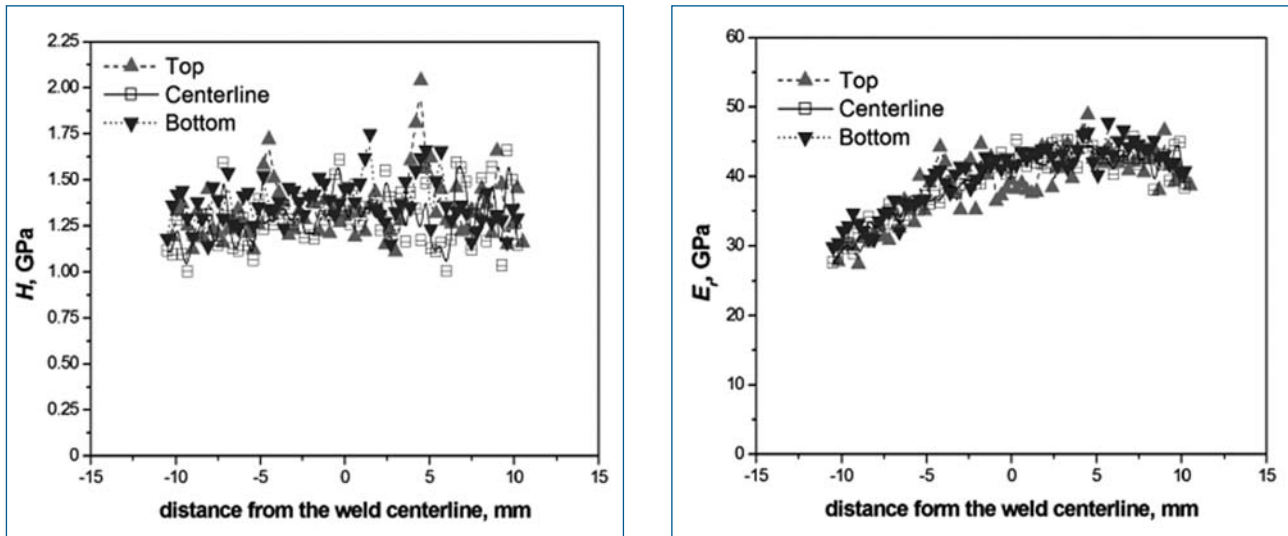


Fig. 5 - a) Hardness profile taken along three sheet section depths: 50 μm from the surface in contact with the shoulder, Top; at centerline; at 50 μm from the surface opposite to the one in contact with the shoulder. b) Local elastic modulus. FSP at $\omega/v = 83 \text{ rev/mm}$.

Fig. 5 - a) Profili di microdurezza rilevati a tre profondità: a 50 μm dalla superficie in contatto con la spalla dell'utensile, Top; al centro; a 50 μm dalla superficie opposta a quella in contatto con la spalla dell'utensile. b) Modulo elastico locale. FSP a $\omega/v = 83 \text{ rev/mm}$.

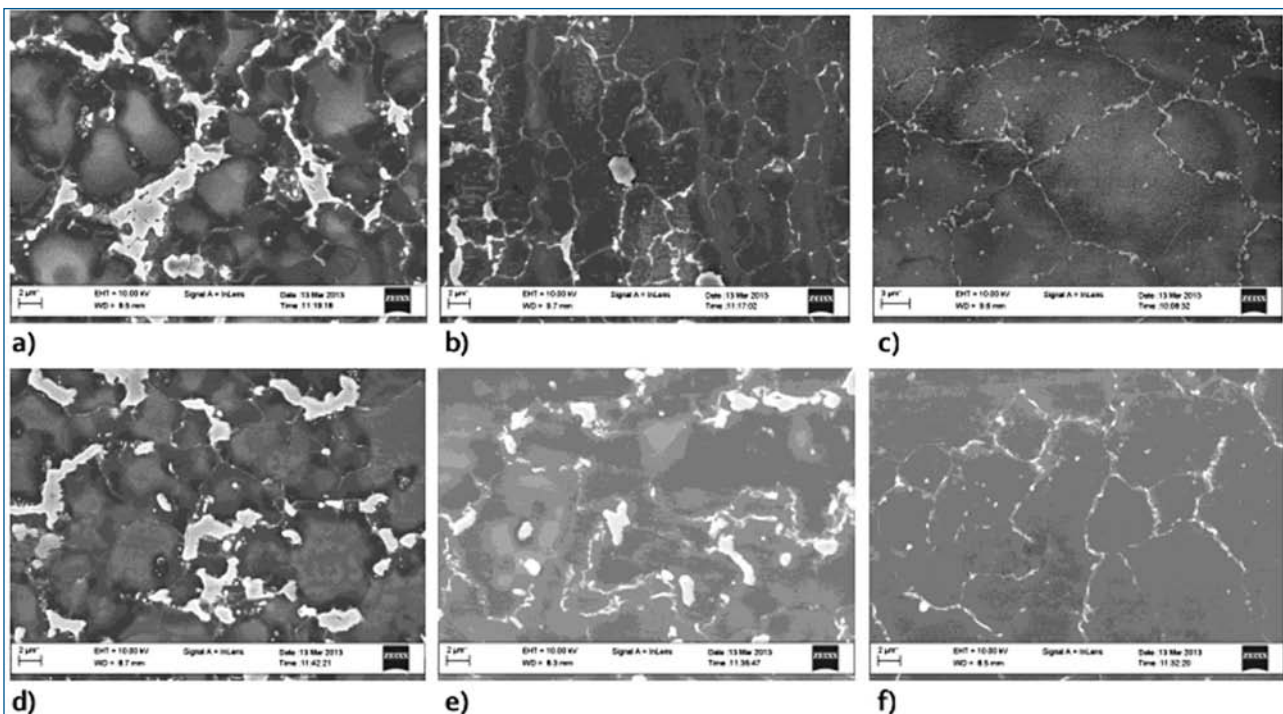


Fig. 6 - FEGSEM of, a) the TMAZ, b) TMAZ/SZ, and c) SZ, of FSP $\omega/v = 50 \text{ rev/mm}$, and, d) TMAZ, e) TMAZ/SZ, and f) SZ, of FSP $\omega/v = 83 \text{ rev/mm}$.

Fig. 6 - Micrografie FEGSEM di, a) TMAZ, b) TMAZ/SZ, e c) SZ, nel campione FSP $\omega/v = 50 \text{ rev/mm}$, e, d) TMAZ, e) TMAZ/SZ, e f) SZ per FSP $\omega/v = 83 \text{ rev/mm}$.

same location of the H measurements of the FSP-1(2500 rpm pin rotation speed, ω , and 50 mm/min traverse speed, v).

The FSP performed at $\omega/v = 50 \text{ rev/mm}$ showed hardness profiles, at the Top, Centerline and bottom depths, having

rather wavy trends, with values oscillating around a mean $H = 1.35 \pm 0.20 \text{ GPa}$ of more than 20. The elastic modulus, E_r increased from $(35 \pm 2) \text{ GPa}$ in the BM to its top value of $46 \pm 2 \text{ GPa}$ at the mid-point of the SZ. At the same time, the TMAZ also experienced higher values, compared to the

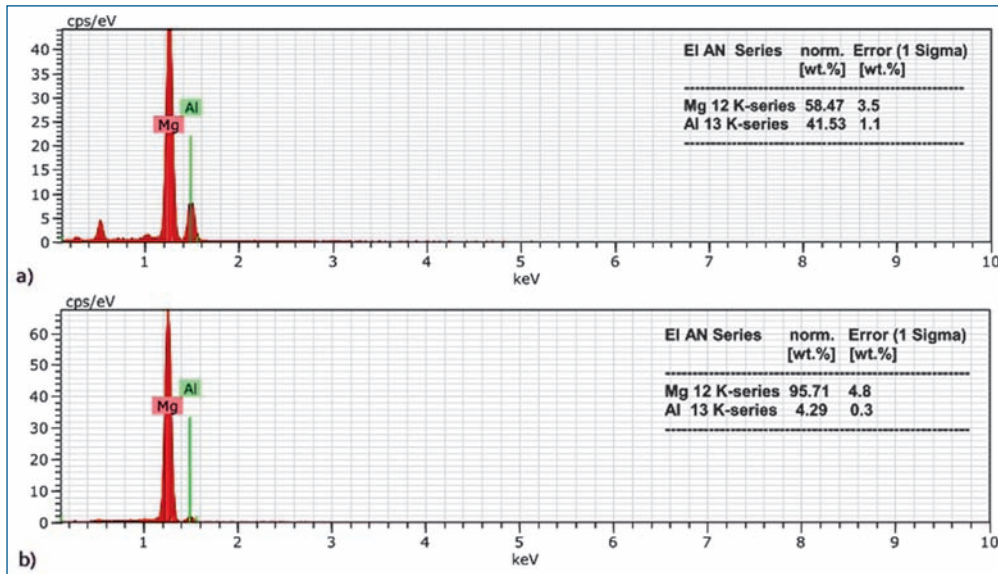


Fig. 7 - Energy-dispersive spectrum (EDS) quantitative analysis of, a) the intergranular phase, and, b) the Mg matrix. The intergranular phase was identified as: $\beta\text{-Mg}_{17}\text{Al}_{12}$.

Fig. 7 - Microanalisi EDS a) della fase intergranulare e b) della matrice di Mg. La fase intergranulare è $\beta\text{-Mg}_{17}\text{Al}_{12}$.

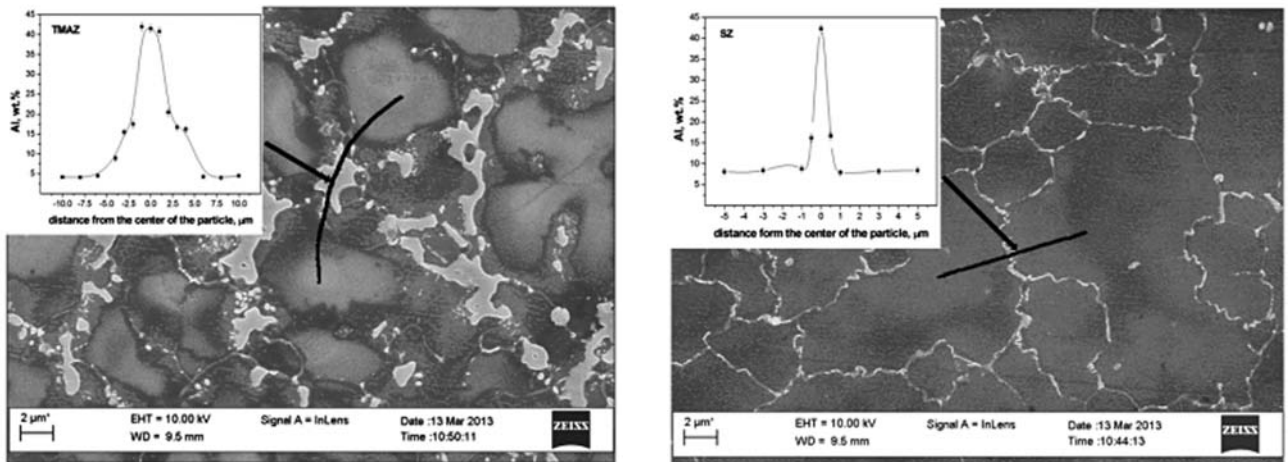


Fig. 8 - EDS analysis of a) TMAZ and b) SZ of FSP $\omega/v = 50$ rev/mm.

Fig. 8 - Microanalisi EDS a) della TMAZ e b) della SZ per il campione FSP $\omega/v = 50$ rev/mm.

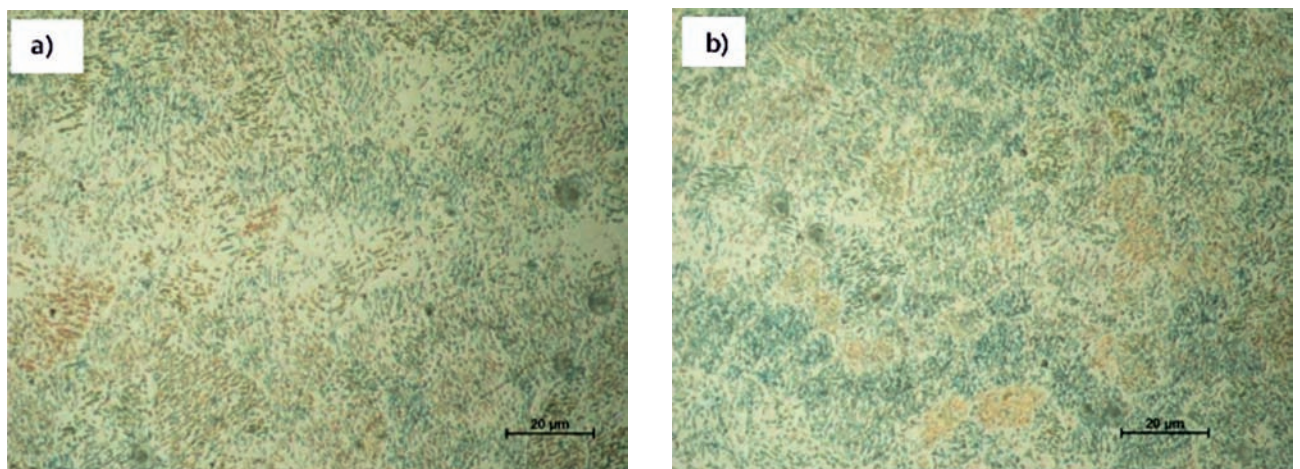


Fig. 9 - LM of precipitates after aging at 300°C (SZs) in a) $\omega/v = 83$ rev/mm and b) $\omega/v = 50$ rev/mm.

Fig. 9 - Microscopia ottica dei precipitati dopo invecchiamento a 300°C (zona SZ) nel campione a) $\omega/v = 83$ rev/mm e b) $\omega/v = 50$ rev/mm.

ones recorded at the BM.

The case of the FSP performed at $\omega/v = 83$ rev/mm is presented in Fig. 5. The mean H at the BM and AS-TMAZ, in all the three section depths, are 1.28 ± 0.15 GPa (Fig. 5a), which is quite similar to, and within the experimental confidence of, the hardness of the $\omega/v = 50$ rev/mm case. Here, as well as the case of the $\omega/v = 50$ rev/mm case, the elastic modulus increased from the BM $E_r = 28 \pm 2$ GPa to the mean $E_r = 34 \pm 4$ GPa of the AS-TMAZ, and to the highest values of $E_r = 40 \pm 2$ GPa, at the SZ. The results show lower H and E_r values measured in the case of $\omega/v = 83$ rev/mm compared to that of $\omega/v = 50$ rev/mm. They can be related to the microstructure evolution induced by the friction stir process at the different characteristic sheet zones: TMAZ, in the AS and RS, and SZ.

EDS analysis

To show further the microstructure modification which occurred at the SZ, FEGSEM inspections were carried out and these are shown in Fig. 6. The intergranular phase, identified by EDS as β -Mg₁₇Al₁₂ (Fig. 7a), is rather coarse and widely spread in the TMAZ (fig. 6a and 6d). On the other hand, the SZ presents well localized and much smaller intergranular β phase particles, in an equiaxed grained structure no longer showing dispersed coarse intergranular β phase (Fig. 6b and 6e). The TMAZ and SZ (Fig. 6c and 6f) of the two FSP ω/v conditions did not show any significant microstructure differences. The magnesium-aluminum ratio significantly increased in the magnesium matrix compared to the intergranular eutectic region (Fig. 7b), due to aluminum being mainly distributed in solid solution within the magnesium matrix. A further investigation was performed by EDS to account for aluminum content variations from inside the intergranular region to the grain center, in both TMAZ and SZ zones (Fig. 8). The aluminum EDS profiles show an Al content of less than 5% inside the magnesium grains of the TMAZ region (Fig. 8a) and 8% of Al, at least in the SZ case. The stirring action and the temperature increase during FSP thinned the intergranular phase and some aluminum went into solid solution. To furthermore investigate this action, an aging treatment at 300°C was performed directly on the FSP samples: light microscopy (fig. 9) shows precipitates uniformly distributed inside the magnesium grains due to the increased level of Al that had existed in solid solution.

In both FSP conditions, both LM and FEGSEM inspections revealed that the SZ grained structure was essentially equiaxed but not homogeneous in size, which accounted for almost one order of magnitude variance from the smaller to the larger grains.

CONCLUSIONS

Friction stir processing at high rotation speeds has been performed on AZ91 high pressure die cast plates to investigate microstructure and mechanical properties. FSP induced the disappearance of porosity in the nugget zone,

that is typical of the HPDC process, but some tunnel defects were introduced. The grain structure, decorated by intergranular eutectic regions in the BM and in the TMAZ, is deeply rearranged into a recrystallized grain structure in the SZ, with no eutectic regions. These latter were dissolved by the FSP stirring deformation before recrystallization. Mean grain sizes in both FSP-1 and FSP-2 SZ were larger in the regions close to the FSPed surface (where the shoulder passed), compared to the centreline and the opposite surface regions. Nanoindentation measurements performed along three parallel lines in the nugget (top, center and bottom) revealed mechanical properties quite comparable at the same distance from the nugget center in the characteristic regions (TMAZ, SZ) of the investigated samples. Subsequent aging at high temperature showed precipitates uniformly distributed inside the magnesium grains, due to the increased level of Al that had been taken into solid solution.

ACKNOWLEDGEMENTS

Authors wish to thank Mr. D. Ciccarelli and Dr. M. Perialisi for their assistance in FSP and LM specimen preparation.

REFERENCES

- [1] R.S. Mishra, M.W. Mahoney, S.X. McFadden, N.A. Mara, A.K. Mukherjee, *Scri. Mater.* 42 (1999) 163–168.
- [2] R.S. Mishra, Z.Y. Ma, *Mater. Sci. Eng. R* 50 (2005) 1–78.
- [3] R.S. Mishra, M.W. Mahoney, in: R.S. Mishra, M.W. Mahoney (Eds.), *Friction Stir Welding and Processing*, ASM International, Materials Park, OH, 2007, pp. 309–350.
- [4] W.M. Thomas, E.D. Nicholas, J.C. Needham, M.G. Murch, P. Templesmith, C.J. Dawes, G.B. Patent application no. 9125978.8, December 1991.
- [5] Z.Y. Ma, *Metall. Mater. Trans. A* 39A (2008) 642–658.
- [6] S.H.C. Park, Y.S. Sato, H. Kokawa, *Metall. Mater. Trans. A* 34A (2003) 987–994.
- [7] W. Woo, H. Choo, D.W. Brown, P.K. Liaw, Z. Feng, *Scri. Mater.* 54 (2006) 1859–1864.
- [8] Z.Y. Ma, A.L. Pilchak, M.C. Juhas, J.C. Williams, *Scri. Mater.* 58 (2008) 361–366.
- [9] U.F.H.R. Suhuddin, S. Mironov, Y.S. Sato, H. Kokawa, C.W. Lee, *Acta Mater.* 17 (2009) 5406–5418.
- [10] W. Yuan, R.S. Mishra, B. Carlson, R.K. Mishra, R. Verma, R. Kubic, *Scri. Mater.* 64 (2011) 580–583.
- [11] V. Jain, J.Q. Su, R.S. Mishra, R. Verma, A. Javaid, M.

- Aljarrah, E. Essadiqi, in: W.H. Sillekens, et al., (Eds.), Magnesium Technology, TMS, Warrendale, PA, 2011, pp. 565–570.
- [12] V. Jain, W. Yuan, R.S. Mishra, Gouthama, A.K. Gupta, Mater. Sci. Forum 702–703 (2012) 64–67.
- [13] W.B. Hutchinson, M.R. Barnett, Scri. Mater. 63 (2010) 737–740.
- [14] S. Celotto, T.J. Bastow, Acta Mater. 49 (2001) 41–51.
- [15] D. Duly, J.P. Simon, Y. Brechet, Acta Metall. Mater. 43 (1995) 101–106.
- [16] K.N. Braszczynska-Malik, J. Alloys Compounds 477 (2009) 870–876.
- [17] W.C. Oliver, G.M. Pharr, J. Mater Res 7 (1992) 1564–1580.
- [18] M. Cabibbo, P. Ricci, R. Cecchini, Z. Rymuza, J. Sullivan, S. Dub, S. Cohen, Micron 43 (2012) 215–222.

Microstruttura e nanoindentazione della lega Mg-Al-Zn pressocolata dopo Friction Stir Processing

Parole chiave: Magnesio e leghe - Microscopia elettronica - Prove meccaniche

Una lega di magnesio ottenuta da pressocolata ad alta pressione (HDPC) è stata sottoposta a Friction Stir Processing (FSP) con elevate velocità di rotazione dell'utensile e differenti velocità di avanzamento. Il processo di FSP induce la scomparsa delle porosità tipiche della HPDC e determina la formazione di fasi molto fini a bordo grano. La caratterizzazione meccanica è stata eseguita localmente tramite nanoindentazione delle zone termomeccanicamente alterate (TMAZ) e severamente deformate (SZ) sia nel lato advancing che retreating, a differenti profondità nella sezione, mentre la caratterizzazione microstrutturale è stata eseguita tramite osservazioni al SEM-FEG con microanalisi delle fasi più rilevanti. La severa deformazione plastica e l'innalzamento della temperatura durante la FSP hanno determinato un incremento della quantità di Al in soluzione solida nei grani di Mg. L'invecchiamento ad alta temperatura eseguito successivamente ha evidenziato una distribuzione uniforme di precipitati all'interno dei grani di Mg.